Eur. Phys. J. D (2021)75:287
https://doi.org/10.1140/epjd/s10053-021-00294-2

THE EUROPEAN PHYSICAL JOURNAL D

Regular Article – Atomic and Molecular Collisions

Ionization and fragmentation of valine molecules in the gas phase by electron impact

A. N. Zavilopulo[1,a], A. I. Bulhakova[1], S. S. Demes[2], E. Yu. Remeta[1], and A. V. Vasiliev[1]

[1] Institute of Electron Physics, National Academy of Sciences of Ukraine, Uzhhorod 88017, Ukraine
[2] Institute for Nuclear Research (ATOMKI), Debrecen 4026, Hungary

Received 25 August 2021 / Accepted 18 October 2021

Abstract. Formation of fragment ions due to single and dissociative ionization of the valine molecule ($C_5H_{11}NO_2$) by electrons was studied by mass spectrometry. This is the first experimental mass-spectrometric measurement of total cross-section in arbitrary units of the valine molecule ionization by electron impact. The experiment was carried out using a setup with an MX-7304A monopole mass spectrometer in the range of mass numbers of 0–120 Da. Mass spectra of the molecules were studied at different vapor temperatures. The results obtained were compared with the mass spectra of the D-, L-, and DL-enantiomeric forms of the valine molecule taken from NIST and SDBS databases. The features of the processes of fragment ion formation of valine molecules by electron impact were analyzed in detail. Dynamics of the fragment ion yield in the range of the initial substance evaporation temperatures of 300–440 K was studied. The ionization potential of the valine molecule was measured (8.72 ± 0.22 eV) and calculated *ab initio* in the adiabatic approximation (9.367 eV). The ionization potential was estimated from the binding energy of the HOMO orbital of the neutral molecule. This is the first calculation of the single ionization cross section of the D-, DL-, and L-forms of this molecule in the Binary-Encounter-Bethe model and using the Gryzinski formula. The experimental cross section values at the threshold are normalized by the theoretical values in absolute units.

1 Introduction

In the process of interaction with a living organism, ionizing radiation can cause various changes in the genotype by acting on the DNA and RNA macromolecules. Penetrating the body, radiation generates fluxes of low-energy secondary electrons with energies from 0.1 to tens of electron volts [1]. Secondary electrons initiate destructive changes in DNA and RNA due to excitation [2,3] and ionization [4], the consequences of which can be estimated by studying information about the most probable channels for fragmentation of these biomolecules.

According to the established concepts [5], the main part of destructive changes at the molecular level of biostructures is associated with slow electrons, with the main target being genetic macromolecules [6]. It is known that in a living cell proteins comprise about half of its dry mass; meanwhile, the whole diversity of proteins in nature is built of 20 amino acids only. Proteins perform a variety of functions, as they serve as molecular tools through which genetic information finds its real embodiment. To build all proteins, whether they are proteins from the most ancient bacteria or higher organisms, the same set of 20 amino acids is used, that are covalently linked to each other in a specific sequence characteristic only for a given protein. Each amino acid, due to the specific features of its side chain, is endowed with a chemical identity [7].

Amino acids are molecules of vital organic compounds that simultaneously contain an amino (-NH_2) and carboxyl (-COOH) groups. They are monomeric units of proteins, in which amino acid residues are linked by peptide bonds. Most proteins are built from a combination of nineteen "primary" amino acids. They contain a primary amino group and a "secondary" amino acid proline or an imino acid (contains a secondary amino group). They are called standard or proteinogenic amino acids [8,9]. The properties of proteins are determined by the characteristics of the constituent amino acids, including such as phenylalanine, proline, histidine, glycine, valine, glutamine, and methionine.

Mass spectrometric and spectral analyses are important methods for studying the structure of matter and the physical processes occurring in it. This work is devoted to a mass spectrometric study of ionization and fragmentation of valine molecules by electron impact.

Valine, an aliphatic α-amino acid, one of the eight amino acids not synthesized in a human body, is crucial for the growth and synthesis of body tissues, muscle coordination, nitrogen exchange, regulation of neural processes, and stabilization of hormone levels [10]. Frag-

[a] e-mail: gzavil@gmail.com (corresponding author)

Published online: 12 November 2021

mentation processes of the valine molecule were studied in a number of works [11–15]: mass spectra of the studied molecules were obtained and possible dissociation channels were proposed. Attention was drawn to the fact that the presence of water molecules reduces the fragmentation efficiency of the initial molecule [14]. Mechanisms and specific features of these processes can be studied not only by optical spectroscopic techniques but also by investigating the interaction of molecules with slow electrons. These methods include electronic mass spectroscopy, that is, a study of mass spectra, temperature dependences of appearance of positive fragment ions, dissociative ionization of amino acid molecules under interaction with low-energy (4–30 eV) electrons, and determination of energies of appearance of ionized fragments. A detailed study of these aspects is undoubtedly a relevant task.

In this paper, we present experimental results on the studies of ionization and fragmentation of the valine molecule in the vapor phase by electron impact as well as compare relative intensities of practically all mass peaks of this molecule with the data from the literature and NIST and SDBS databases. A detailed analysis of processes of formation of fragment ions in the mass spectra enables the effect of structural forms of valine enantiomers on the redistribution of the product ion relative intensities to be shown. Theoretical calculations of the geometry and electron structure of three forms (D-, DL-, and L-) of the valine molecule and its single-charged positive ion enabled the single ionization cross sections for these forms to be obtained. Normalization at the threshold of the experimental total cross section by the theoretical value provided important data on the process cross section in absolute units.

2 Experimental setup

The experiment was performed using a setup with an oil-free pumping unit described in detail earlier [4,16]. An MX-7304A type monopole mass spectrometer was used as an analytical instrument. The range of the recorded masses is 1–120 Da, with a mass resolution not worse than $\Delta M = 1$ Da. The ion source of the mass spectrometer was operating in the electron current stabilization mode enabling an electron beam with an energy controlled from 5 to 70 eV to be produced. The following modes of operation of the electron source are possible:

- Measurement of mass spectra in a fixed energy mode in the range of 10–90 eV.
- Measurement of energy dependences with a smooth energy variation within 5–70 eV.

The electron current can be varied within the range of 0.05–0.5 mA, while the minimum energy spread $\Delta E_{1/2} = 250$ MeV, where this value is the full width at half maximum of the electron energy distribution. Ions, formed as a result of interaction with electrons, are mass-separated, detected, and recorded by a measuring system with a digital indication of the particle mass number and intensity, with manual, cyclic, or programmed variation of the mass spectrum and the bombarding electron energy. A beam of neutral molecules is created by a channel source of effusive type, which provides a concentration of molecules in the area of interaction with the electron beam in the range of 10^{-10}–10^{-11} cm^{-3}. A special controller with feedback provided a highly stable heating temperature in the 300–600 K range. The mass scale was calibrated using Ar and Xe beams, and the control mass spectra were measured for freon, sulfur hexafluoride, and krypton. The energy scale was calibrated using the initial part of the ionization cross section of the Kr atom, which enabled the electron energy to be determined with an accuracy not worse than ± 0.08 eV.

Measurements of the mass spectra of the valine molecule (Valine Powder from Myprotein) were carried out at different energies of the ionizing electrons. The experiment was performed in two stages: at the first stage the mass spectra in the range of 1–120 Da were thoroughly measured at the ionization energies E_i of 20, 30, 40, 50 and 70 eV while at the second one relative total ionization cross section of valine molecule at the incident electrons energy of 5–60 eV were investigated. The registration and data processing were carried out in automatic mode using special software.

The measurement technique was reduced to the simultaneous measurement of fragment ions; for this, the energy range was initially set, then the investigated masses were set (no more than 20), and the total measurement time was calculated by the formula

$$T_{\text{full}} = t_1 \cdot n \cdot C, \tag{1}$$

where t_1 is the measurement time of one fragment, n is the number of fragments, C is the number of cycles which was determined depending on the value of the useful signal.

Registration and processing of the experimental results were carried out in an automatic mode using special computer programs.

3 Results and discussion

In Fig. 1 structural diagrams of the $C_5H_{11}NO_2$ molecule and enantiomers of the L-, DL-, and D-forms are shown. It is known [7] that valine belongs to the group of simple aliphatic non-polar α-amino acids which have the largest alkyl side chain Cα. It should be noted that aliphatic amino acids can be considered as model systems in the processes of interaction of ionizing radiation with larger biomolecular complexes (proteins, peptides). Primary ionizing radiation produces secondary particles, such as radicals or electrons with energies below 20 eV that play an important role in generating defects in a biological system. The energy of

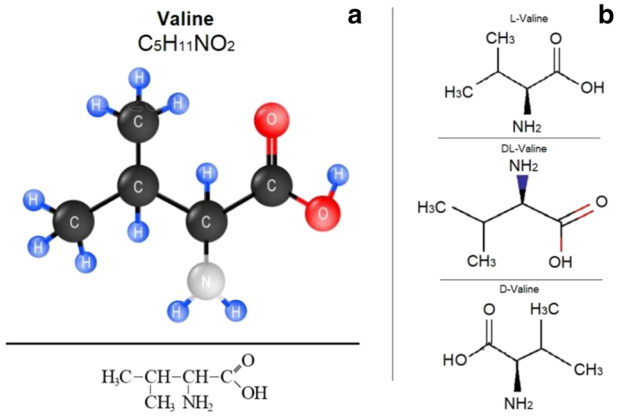

Fig. 1 Structural formulas of valine (**a**) and its enantiomers of L-, DL-, and D-forms (**b**)

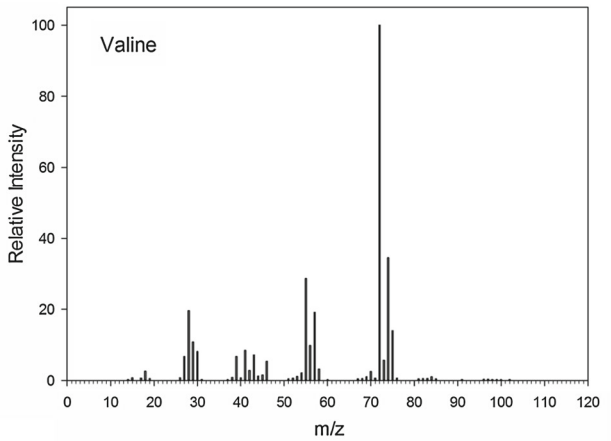

Fig. 2 Mass spectrum of the D-valine molecule. Electron energy $E = 70$ eV, temperature $T = 393$ K

the secondary electrons is sufficient to cause dissociation and/or electron ionization processes directly in the medium. This initiates additional damage to the structure. The maximum negative charge in amino acids is, as a rule, localized on oxygen atoms belonging to the carboxyl group while the positive charge is localized on all hydrogen atoms.

As can be seen from Fig. 1, a distinctive feature of the valine molecule is the presence of hydrogen atoms, connected with 4 substituents. The first one is a hydrogen atom, the second one is a carboxyl group COOH, the third one is an amino group NH_2 which is capable of attaching a hydrogen ion, the fourth one is an alkyl group, the side chain of Cα atoms, its composition determines the basic properties of this amino acid. The valine enantiomers should possess similar energy characteristics: ionization potentials, heat of formation, activation energies, and mass spectra of fragments formed at the dissociation of the molecular ions. The enantiomers differ only in vector characteristics which determine the molecule properties depending on its structure [17,18].

Amino acid molecules exist in the form of various conformers; in addition, they have L-, DL-, and D-forms (Fig. 1). There are two types of amino acid isomerism: structural, related to the structure of the carbon skeleton and relative position of functional groups, and optical (spatial) isomerism. Since α-amino acids contain an asymmetric carbon atom (Cα-atom), they can exist in the form of optical isomers (mirror antipodes) which play an important role in the processes of protein biosynthesis.

The carboxyl group can rotate, and the hydrogen atom can be oriented both in the nitrogen direction and in the opposite direction. Moreover, the conformational variability of the molecules contributes to the reorientation of the flexible carboxyl (-COOH) and amine (-NH_2) groups (Fig. 1), forming various intramolecular hydrogen bonds. For example, a bond of nitrogen atom lone pair with a hydrogen of the hydroxyl group (N...HO), or a bond between the hydrogen atom of the amine group and the oxygen atom of the carbonyl (NH...O=C) and hydroxyl (NH...OH) groups.

3.1 Mass spectra

Figure 2 shows the mass spectrum (MS) of a D-valine molecule (Sigma-Aldrich, purity 0.999, № CAS72-18-4) in the mass range 0–120 Da, obtained at the molecule source temperature of 393 K and the ionizing electron energy $U_e = 70$ eV. As can be seen, four groups of lines, in which the highest intensity belongs to ions with $m/z = 28, 42, 56$ and 72, respectively, are clearly distinguished in the MS. The peak of the parent ion ($m/z = 117$) is practically absent in the spectrum, which is characteristic of the mass spectra of aliphatic amino acids [19] and is due to the low stability of the molecular ion formed during the ionization. Typically for most α-amino acids, the main channel of dissociation of the valine molecule under electron impact is due to the rupture of the C–Cα bond, which results in the formation of an ion with mass $m/z = 72$ due to the detachment of a neutral carboxyl group COOH (Fig. 1).

As follows from Fig. 1, the enantiomers of the valine L-, DL-, and D-forms are structurally very different, this can be revealed in the mass spectra as a redistribution of relative intensities. This statement can be confirmed by comparing the available data for these enantiomers, as well as by calculating binding energies for them.

Such comparison of our data of the relative intensities of mass peaks of the valine molecule from the NIST databases [20], SDBS [21], and obtained at electron and photon impact in Refs. [11,14,22,23] is shown in Table 1. Comparison of the relative intensities of the mass peaks of fragments during electron and photon impacts shows similar values. Difference in the relative intensities for some production ions is most likely related to the specific features of reactions of the fragment ion formation at electron-molecule and photon-molecule interaction [14,22].

Table 1 Comparison of relative intensities of the mass peaks of the valine molecule ($C_5H_{11}NO_2$) fragments obtained by different methods

m/z	Ion assignments	NIST [20]		SDBS [21]				Electron impact 70 eV				Photon impact 20 eV	Our data D-
		DL-	D-	DL-	L-	DL-Nor	D-	[23]	[14]	[11]	[22]	[22]	
2	H_2^+			0.1	0.15								0.12
14	CH_2^+	0.2		0.2	0.14	0.1	0.1	0.36					0.14
15	CH_3^+	0.7		0.7	0.9	1.1	1.2	2.24					0.92
16	NH_2^+				0.1			0		0.11			0.12
17	NH_3^+ (OH^+)	0.6		0.6	0.61	0.2	0.5	0.72					0.61
18	NH_4^+	2.6		2.6	3.76	3.7	3.2	4.32	2.8	1.64	4		3.74
19	OH_3^+	0.5		0.5	0.5	0.3	0.6	1.08		0.26			0.5
26	$C_2H_2^+$	0.7	1.31	0.7	1.09	0.8	0.7	2.52		0.27			1.09
27	$C_2H_3^+$	6.7	11.3	6.7	5.5	6.1	7.4	9.36	9.66	6.79	9	6	5.5
28	CH_2N^+ (CO^+)	19.6	18.2	19.6	20.61	14.9	24.7	30.6	32.8	12.54	31	36	20.61
29	CH_3N^+ (CHO^+)	10.8	10.1	10.8	11.31	5.3	14.2	20.52	21.0	10.01	21	36	11.31
30	$NH_2CH_2^+$	8.1	12.6	8.1	9.9	10.5	10.5	12.24	14.8	6.43	12	19	9.92
31	CH_3O^+	0.2	0.5	0.2	0.3	0.7	0.2	0.36		0.63			0.33
32	CH_3OH^+	0.1		0.1	0.2	0.2	0.3	–		0.21			0.23
33	$CH_3OH_2^+$	0.1		0.1	0.1	0.1		–					0.11
36	$CH_6OH_2^+$				0.4		0.4						0.43
37	C_3H^+	0.2	0.5	0.2	0.25	0.2		–					0.25
38	$C_3H_2^+$	0.8	1.2	0.8	0.71	0.6	0.5	–		0.71			0.71
39	$C_3H_3^+$	6.7	8	6.7	6.35	3.5	7.2	7.56	9.4	4.69	8	3	6.35
40	$C_2H_2N^+$	0.7	3.3	0.7	1.05	0.6	0.9	1.44		0.74			1.05
41	$C_2H_3N^+$ ($C_3H_5^+$)	8.4	12.6	8.4	8.21	3.7	8.7	8.28	9.9	6.43	8	9	8.21
42	$C_2H_4N^+$	2.8	5.9	2.8	3.49	4.9	3.1	3.96	4.0	2.54	4		3.49
43	NH_3CHCH^+ ($C_3H_7^+$)	7.2	10.5	7.2	7.04	4.7	6.7	6.84	7.7	4.98	7	13	7.03
44	$NH_3CHCH_2^+$	1.2	7.7	1.2	2.97	7.8	1.6	2.16		2.43			2.97
45	$COOH^+$	1.5	5.1	1.5	2.1	1.6	2.1	2.88	3.0	1.38	3	6	2.1
46	NH_2CHOH^+	5.4	5.1	5.4	5.3	3.1	6.4	5.4	10.0	3.6	5	13	5.3
47	$NH0_2^+$		0.2		0.2			0.36		0.22			0.2
49	$NH_30_2^+$	0.1		0.1	0.1			1.8					0.1
50	$NH_40_2^+$	0.1		0.1	0.14	0.2	0.2	–					0.14
51	NC_3H^+	0.4	0.5	0.4	0.36	0.2	0.4	–					0.36
52	$NC_3H_2^+$	0.6	0.7	0.6	0.52	0.2	0.6	–					0.52
53	C_3HO^+	1.1	1.5	1.1	1.1	0.6	1.2	–					1.1
54	$C_3H_2O^+$	2.1	2.5	2.1	1.84	0.8	1.9	1.8					1.84
55	$C_3H_3O^+$	28.7	24.9	28.7	26.33	6.1	31.4	30.24	38.0	28.91	30	64	26.33
56	$C_3H_4O^+$	9.8	12.2	9.8	9.86	3	12	11.16	14.8	5.46	11		9.86
57	CH_3NCOH^+	19.1	26.7	19.1	20.48	3	24.5	29.04	23.2	26.08	29	60	20.48
58	$C_2H_6CO^+$	3.2	3.9	3.2	2.9	0.1	3.3	–		1.96			2.9
59	$C_2H_5NO^+$		0.5		0.28		0.2	–		0.29			0.28
60	$C_2H_5NOH^+$	0.2	0.5	0.2	0.22		0.1	–					0.22
67	$C_5H_7^+$	0.4	0.6	0.4	0.31		0.2	–					0.31
68	$C_5H_8^+$	0.5	1	0.5	0.44	0.2	0.3	–					0.44
69	$CH_3CHCHCHCH_3^+$	1	2.1	1	0.77	0.1	0.4	–					0.77
70	$CH_3CH_2CHCHCH_3^+$	2.5	2.9	2.5	2.16	1.1	2.1	1.44		1.78			2.16
71	$C_2HNO_2^+$	0.6	1	0.6	0.57	0.2	0.6	0					0.57
72	$C_2H_2NO_2^+$	100	100	100	100	100	100	100	100	100	100	100	100
73	$C_2H_3NO_2^+$	5.7	5.3	5.7	5.28	4.9	5	5.04		5.66			5.28
74	$C_2H_4NO_2^+$	34.5	13.2	34.5	30.46	24	34	33.84	30.2	35.82	34	45	33.46
75	$C_2H_5NO_2^+$	14	8.6	14	12.35	2.1	15.3	15.84	11.4	13.67	16	12	12.35
76	$C_2H_6NO_2^+$	0.6	0.5	0.6	0.43	0.1		0.72		0.42			0.43
77	$C_2H_7NO_2^+$				0.13		0.1	–					0.13

Table 1 continued

m/z	Ion assignments	NIST [20]		SDBS [21]				Electron impact 70 eV				Photon impact 20 eV	Our Data D-
		DL-	D-	DL-	L-	DL-Nor	D-	[23]	[14]	[11]	[22]	[22]	
78	$C_2H_8NO_2^+$	0.1		0.1	0.12		0.1	–					0.12
79	$C_2H_9NO_2^+$	0.1		0.1	0.14			–					0.14
81	$C_4H_3NO^+$	0.4		0.4	0.28		0.1	–					0.28
82	$C_4H_4NO^+$	0.5	0.8	0.5	0.41	0.1	0.3	–		0.37			0.41
83	$C_3HNO_2^+$	0.5	1	0.5	0.44		0.2	–					0.44
84	$C_4H_8N_2^+$ ($C_3H_2NO_2^+$)	1	1	1	0.96		0.8	0.72					0.96
85	$C_3H_3NO_2^+$	0.4	1.5	0.4	0.54		0.3	–		1.11			0.54
88	$NH_2CH_2CHCOOH^+$		0.5		0.43	0.3		–					0.43
91	C_5HNO^+	0.2		0.2	0.23			–					0.23
92	$C_5H_2NO^+$	0.1		0.1	0.11			–					0.11
93	$C_5H_3NO^+$	0.1		0.1	0.13			–					0.13
95	$C_5H_5NO^+$	0.1		0.1	0.12			–					0.12
96	$C_5H_6NO^+$	0.3		0.3	0.34			–					0.34
97	$C_5H_7NO^+$	0.3		0.3	0.22		0.1	–					0.22
98	$C_5H_8NO^+$	0.2	0.6	0.2	0.27		0.3	–					0.27
99	$C_5H_9NO^+$	0.2	1	0.2	0.28			–					0.28
101	$NH_5CHC0_2C_2H^+$	0.2	1.8	0.2	0.42		0.1	–					0.42
102	$NH_6CHC0_2C_2H^+$	0.2	0.3	0.2	0.28		0.3	–					0.28
117	$NH_2(CH_3)_2(CH)_2COOH^+$		0.2		0.25			0.1	0.1		0.1	1	0.12
118	$NH_3(CH_3)_2(CH)_2COOH^+$		0.3		0.33		0.25	–	0.2				0.17

The results of the study of the mass spectra of the enantiomers L-, DL-, and D- forms of the valine molecule obtained in different laboratories give the most complete picture of the fragment ion formation processes. The comparison of the relative intensities in Table 1 shows a satisfactory agreement. However, some differences are observed: not in all cases ions with $m/z = 2, 16, 34, 36$ are revealed, relative peak intensities for the formation of fragment ions with masses m/z = 28, 29, 57, 58 differ for the L-, DL-, and D-enantiomers (see Table 1). As noted above, the enantiomers should have the same mass spectra of fragment ions formed at the dissociation of molecular ions [18]. However, analysis of the available data on the mass spectra of fragments formed during the ionization of amino acids by electron impact reveals significant differences for several D- and L-amino acids [17,18,22]. These differences, obviously, can be related only to different probabilities of formation of fragments (see Fig. 1b).

Analysis of the obtained mass spectra allows us to conclude on the mechanisms of the formation of the most intense fragment ions at dissociative ionization by electron impact. As noted above, ionization and removal of an electron lead to a weakening of bonds in a molecular ion compared to a neutral molecule. For all optimal structures of the parental cations of amino acids, positive charge is mainly localized on the carbon atom of the carboxyl group, and in the process of dissociation, the charge is transferred to the carbon chain. As follows from the mass spectrum and data of Table 1, the $COOH^+$ peak ($m/z = 45$) has low intensity (Fig. 2). Let us consider the processes leading to the formation of the most intense fragment ions.

m/z = 72. This is the main fragment ion peak since it is the most intense for all enantiomers which arise as a result of effective dissociation of the parent ion of the valine molecule due to a breakdown of the C–C bond with the formation of a neutral carboxyl group fragment COOH (Fig. 1a) in accordance with the reaction:

$$C_5H_{11}NO_2 + \quad e^- \rightarrow NH_2(CH_3)_2(CH)_2^+ + (COOH) + 2e^-. \tag{2}$$

m/z = 74. The ion with this mass has a peak with an intensity of 33% of the main one and is related to the dissociation of the side chain (Fig. 1) and formation of propyl C_3H_7:

$$C_5H_{11}NO_2 + e^- \rightarrow NH_2CHCOOH^+ + (CH_3)_2CH + 2e^-. \tag{3}$$

m/z = 57. The appearance of a rather intense peak (20% of the main maximum) at this mass is related to the dissociation of the amino group and formation of neutral molecules of water and propylene C_3H_6:

$$C_5H_{11}NO_2 + e^- \rightarrow NHCHC(OH)^+ + H_2O + CH_3CHCH_2 + 2e^-. \tag{4}$$

m/z = 39, 41, 43. These peaks refer to hydrocarbon ions and the amino and carboxyl groups do not participate in the formation of these fragments:

$$C_5H_{11}NO_2 + e^- \rightarrow CHCHCH^+ + C_2H_6NO + H_2O + 2e^- \tag{5}$$

$$C_5H_{11}NO_2 + e^- \rightarrow CH_2CCH_3^+ + C_2H_5NO_2 + H + 2e^- \quad (6)$$

$$C_5H_{11}NO_2 + e^- \rightarrow (CH_3)_2CH^+ + NH_2CH_2 + CO_2 + 2e^-. \quad (7)$$

m/z = 27, 28, 29, 30. An unambiguous assignment of the peaks of this group is encumbered by the alternative character of appearance of neutral fragments manifested as different intensities of mass peaks obtained at the interaction with electrons and photons (Table 1). For example, the occurrence of the $m/z = 28$ peak can correspond to isobaric CO^+ and CH_2N^+ ions in accordance with the following reactions:

$$C_5H_{11}NO_2 + e^- \rightarrow CO^+ + NH_2CH(OH)CH(CH_3)_2 + 2e^- \quad (8)$$

or

$$C_5H_{11}NO_2 + e^- \rightarrow NHCH^+ + COOH + CH_3CH_2CH_3 + 2e^-. \quad (9)$$

Preference should be given to reaction (9) since the formation of this particular HC-NH fragment is dominant in the processes of dissociation of amino acid molecules [4].

Analysis of the processes of interaction of an electron with the valine molecule under study suggests that separation of the carboxyl COOH group initially occurs as a result of a simple breakdown of the bond between the C1–C2 atoms. The result is the formation of the most intense main peak in the mass spectrum with $m/z = 72$. The process of separation of the whole carboxyl group energetically is very close to the process of detachment of two neutral fragments: H and CO_2. The latter process is energetically more favorable than the detachment of two neutral fragments OH and CO [24].

It should be noted that for the mass range $m/z = 2 - 20$ the explanation of the appearance of peaks in the mass spectrum is rather complicated due to possible alternative channels of dissociative ionization. This is especially true for the peak with $m/z = 2$ detected in the present study and Ref. [21] for the enantiomers of the L- and DL-forms (Table 1).

Note that protonated parental cation $NH_3(CH_3)_2(CH)_2COOH^+$, the intensity of which is not higher than 1%, can be revealed only at certain conditions. One possible, but, evidently, hardly probable channel of formation of this cation is the ion-molecule reaction directly in the ion source. A more probable channel is the presence of H_2 dimers in the molecular beam source, which ionize and dissociate in the area of interaction with the electron beam, forming the $NH_3(CH_3)_2(CH)_2COOH^+$ ion (m/z = 118) and corresponding neutral fragments [14].

Comparison of the relative intensities of the measured mass peaks with data from Refs. [11,14,20–23] (Table 1) in general shows a satisfactory agreement. Note that the evaporation temperature of the valine molecules is given only in Ref. [25] which could introduce corrections in the mass peak intensities. However, a more thorough analysis of the available mass spectra of fragments formed during the ionization of amino acids by electron impact reveals significant differences for several D- and L-amino acids [18,21,22]. In this case, noticeable differences are observed in the mass spectra of the fragment ions of compounds used by the authors of Ref. [25] to identify 2,3-diaminopropanoic acid. A more complete analysis of the processes involving theoretical calculations of the energies, lengths, and orders of bonds of parent and child fragment ions and neutral molecules should be a result of a separate study similar to that carried out in Ref. [22] for photoionization processes.

The above analysis, apparently, does not provide a complete description of the processes of ionization and fragmentation of valine molecules in the gas phase by electron impact. A more complete consideration and analysis of these processes with the account of the fragment chemical composition and the presence of conformers requires extensive theoretical calculations of the energies, lengths, and binding energies for the parent and produced fragment ions and neutral molecules and should comprise a separate study similar to the one performed in Ref. [26,27]. Probably, such theoretical analysis will enable one to explain the difference of intensities at the formation of the fragments with m/z = 55, 56, 75 compared to m/z = 39, 41, 46.

3.2 Temperature dependences

The temperature of amino acid molecules in the gas phase is an important factor affecting processes of their interaction with electrons, especially dissociation with ionization [28–30]. We measured the temperature dependences of the yield of positive fragment ions of the D-valine molecule at an electron energy of 70 eV. As an example, Fig. 3 shows such dependences for the most intense fragment ions $NH_2(CH_3)_2(CH)_2^+$ (m/z =72), $NH_2CHCOOH^+$ (m/z =74), $NHCHC(OH)^+$ (m/z =57), $(CH_3)_2CH^+$ (m/z =43), $CH_2CCH_3^+$ (m/z =41), CNH_2^+ (m/z =28), and CH_3 (m/z =15). The temperature behavior of the curves is generally similar, exhibiting four main sections: at the initial section the behavior of the intensity shows an almost linear growth, then the growth becomes close to exponential, followed by saturation in the temperature range of 400–418 K and a rather sharp decline related to the onset of decomposition of the substances under investigation as well as their fragments. The features in the measured dependences namely change in the slope of the curves at certain temperatures, apparently, should be attributed to the processes (2)–(9) described above.

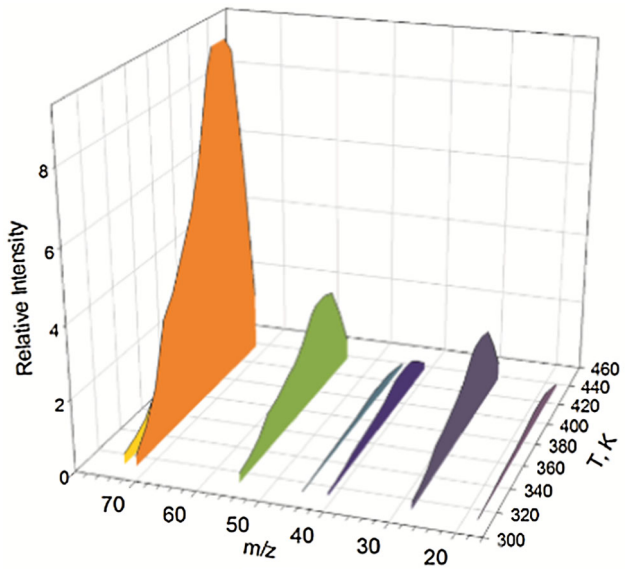

Fig. 3 Temperature dependences of formation of positive fragment ions of the D-valine molecule. The electron energy is 70 eV

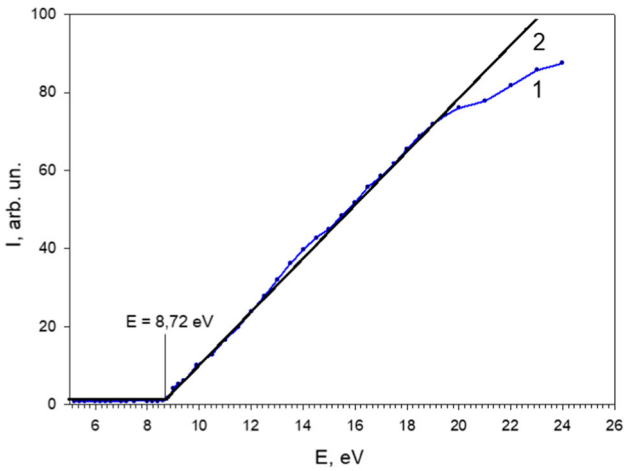

Fig. 4 Energy dependence of total ionization cross section of the D-valine molecule near-threshold region, **1**—experiment, **2**—approximation

3.3 Energy dependence of the total relative ionization cross section

At zero potentials on the deflecting electrodes of the mass spectrometer, the total current of positive ions to the collector was measured. This current is formed as a result of the interaction of the studied valine molecules with electrons. By smooth variation of the energy of ionizing electrons, one can obtain an energy dependence of the total relative cross section of formation of positive ions in a given range of electron energies.

Figure 4 shows the energy dependence of the total relative ionization cross section of the valine molecule in the energy range of 5–24 eV. It also shows the threshold section of this dependence which was used for the least-square approximation [4,28]. As can be seen, the results of the fitting correlate well with the experimental curve, which enables the ionization energy of the valine molecule to be determined as $E_{\mathrm{IE}} = 8.72 \pm 0.22$ eV. Table 2 provides a comparison with the data of other authors.

3.4 Calculation of the ionization potentials of the D-, DL-, L-forms of the valine molecule

Calculations of geometric and electronic structures of three forms (D-, DL-, and L-) of the valine molecule and its single positive ion were carried out using the GAUSSIAN software [35] and the density functional theory (DFT) approximations. The method of such calculations is described in Refs. [36–38]. We used the standard Gaussian Dunning basis set of the aug-cc-pVDZ type with the exchange-correlation functional of the B3LYP type. The geometric structures of the D-, DL-, and L- isomers of the valine molecule and their positive ions were optimized using the quadratic approximation algorithm from the GAUSSIAN program. To calculate the initial geometry of the molecule, equilibrium interatomic distances were specified from the PubChem database [39–41].

Calculations of the ionization potentials of the considered forms of valine molecules were performed *ab initio* in two DFT approximations. In the first, adiabatic, approximation, the ionization potential is equal to the difference between the total energies of the ground states of the parent ion $E_t[\mathrm{Val}^+]$ and the neutral molecule $E_t[\mathrm{Val}]$: $I(\mathrm{Val}) = E_t[\mathrm{Val}^+] - E_t[\mathrm{Val}]$. The states of molecules and their ions in this case correspond to the calculated equilibrium interatomic distances.

In the second, simpler approximation, the value of the ionization potential of a molecule can be approximately estimated from the calculation of the energy characteristics of molecular orbitals. In this approximation, the lower unoccupied (LUMO) and higher occupied (HOMO) molecular orbitals of the molecule are calculated. The binding energies E_{b} of these orbitals make enable one to determine (according to the Koopmans' theorem) the ionization energy (potential) of the molecule and its energy affinity E_{a} to an electron. It follows from the binding energy of an electron in the HOMO orbital that $\mathrm{I(Val)} = -E_{\mathrm{b}}^{\mathrm{HOMO}}(\mathrm{Val})$ while from the binding energy in the LUMO-orbital $E_{\mathrm{a}}(\mathrm{Val}) = -E_{\mathrm{b}}^{\mathrm{LUMO}}(\mathrm{Val})$.

Table 3 shows the total energies calculated here for three forms of neutral valine molecules, their singly charged positive ions, and the calculated adiabatic ionization potentials I (Val) using the DFT approximations. It also lists the binding energies of the HOMO and LUMO orbitals of the mentioned forms of the neutral valine molecule. From Table 3 one can see that the total energies of all forms of the valine molecule are close. A similar relationship between the total energies is also valid for one-charge positive valine ions. This leads to almost the same values of I (Val) for these forms of the molecule in both the adiabatic and molecu-

Table 2 Ionization energy values (eV) of the valine molecule obtained by experimental and theoretical methods

Experiment					Theory		
Electron impact				Photons	G3MP2	OVGF	OVGF
Our data	[31]	[32]	[11]	[22]	[22]	[33]	[34]
8.72 ± 0.22	8.71	9.86	8.91 ± 0.05	8.9	8.89	9.54	9.50

Table 3 Energy characteristics D-, DL-, and L-form of valine molecule

D-, DL-, and L- forms of valine (Val, $C_5H_{11}NO_2$)			
Energy	D-Val	DL-Val	L-Val
Adiabatic approximation			
E_t[Val], a.u.	− 402.528375	− 402.528370	− 402.528231
$E_t[Val^+]$, a.u.	− 402.184155	− 402.184129	− 402.184310
I(Val), eV	9.367	9.367	9.359
Molecular orbital approximation			
E_b^{HOMO}(Val), a.u.	− 0.253093	− 0.25311	− 0.253300
I(Val), eV	6.887	6.888	6.893
E_a(Val), eV	0.594	0.594	0.587
Experiment, eV			
8.72 ± 0.22			

lar orbitals approximations. As can be seen, the value of I(Val), calculated in a more accurate adiabatic approximation, exceeds the experimental value by 0.65 eV while the value estimated from the HOMO orbital is by ∼ 1.83 eV less than the experimental value. Note that the value I(Val) calculated here agrees with the measured and calculated values from Refs. [22,32–34] given in Table 2. Apparently, an improvement in the calculation method due to a more complete account of the electron–electron interaction will make it possible to refine the adiabatic values of the ionization potentials and obtain more realistic values of the HOMO and LUMO orbitals energies.

3.5 Calculation of cross section for one-electron ionization of the valine molecule

Despite the existence and development of certain theoretical methods [42–44], description of elementary processes involving molecules is a rather difficult task. The greatest difficulty consists in investigation of interaction of low-energy electrons with molecular targets. In these processes, an incident electron excites rotational, vibrational, and electronic states of the molecules. At energies above the ionization threshold, collision with electron results in direct or dissociative ionization. Such processes are very complex and often interrelated. Simplified models and approximations are often used.

To estimate the cross section for one-electron ionization of the valine molecule over molecular orbitals taken into account, we used the Binary-Encounter-Bethe (BEB) model [45–47] and the classical Gryzinski approximation (Gryz) [48]. The cross section for ionization of an electron from a molecular orbital in the BEB model has the form

$$\sigma_i(t) = \frac{S}{t+u+1} \cdot \left\{ \frac{1}{2} Q \cdot \left(1 - \frac{1}{t^2}\right) \cdot \ln t + (2-Q) \cdot \left[\left(1 - \frac{1}{t}\right) - \frac{\ln t}{t+1} \right] \right\}. \quad (10)$$

Here $t = T/B$, T is the kinetic energy of an incident electron, B is the binding energy of an electron removed from a molecular orbital, $u = U/B$ where U is the average kinetic energy of electrons at an ionizable molecular orbital, $S = 4\pi \cdot a_0^2 \cdot N \cdot (R/B)^2$, $Q = \frac{2 \cdot B \cdot M_i^2}{N \cdot R}$, $M_i^2 = \frac{R}{B} \cdot \int_0^\infty \frac{1}{w+1} \cdot \frac{df(w)}{dw} dw$, $w = W/B$, where W is the kinetic energy of the removed electron. The function $df(w)/dw$ is the differential oscillator strength of the molecule and N is the number of electrons in the molecular orbital. Constants R =13.6058 eV (Rydberg constant), $a_0 = 5.2918 \cdot 10^{-11}$ m (Bohr radius). We assume that Q =1 [45].

The expression for the cross section of ionization from the molecular orbital in the Gryzinski approximation has the form:

$$\sigma_i(t) = \frac{\sigma_0}{B^2} \cdot \frac{1}{t} \cdot \left(\frac{t-1}{t+1}\right)^{3/2} \cdot \left\{ 1 + \frac{2}{3} \cdot \left(1 - \frac{1}{2t}\right) \cdot \ln \left[2.7 + (t-1)^{1/2} \right] \right\} \quad (11)$$

where: $\sigma_0 = 6.56 \cdot 10^{-14}\, eV^2 \cdot cm^2$. As can be seen, the cross section in this approximation is determined only by the binding energy B of the electron in the molecular orbital.

Characteristics of the molecule structure, binding energy B, the average kinetic energy of electrons U,

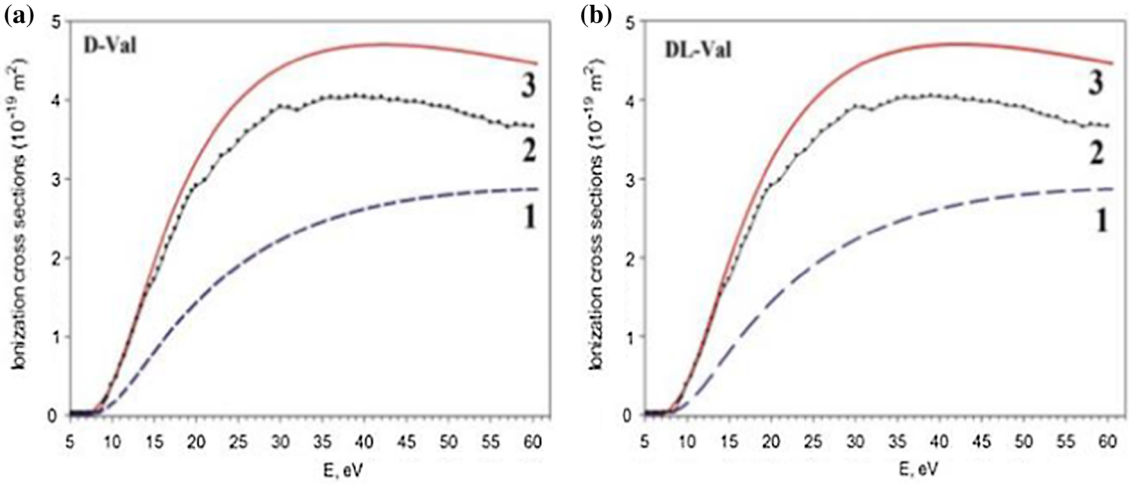

Fig. 5 Ionization cross sections of the D- and DL-forms of the valine molecule. Calculated cross sections of one-electron ionization: BEB-DFT (1), Gryz-DFT (3). Experimental total ionization cross section of D-valin molecule normalized to the BEB-DFT calculation at an energy of 8.8 eV (2)

and several electrons N in the ionized subshell were calculated in the DFT approximation.

These values, calculated in the DFT approximation (BEB-DFT) are very similar for the three forms of the valine molecule. This leads to the close values of the corresponding cross sections of one-electron ionization (see also the energies in Table 3 and the discussion in Ref. [18]). For each form of the molecule, the ionization cross section was calculated from 24 orbitals with binding energies up to 200 eV, which contain 2 electrons each. For example, in the DFT approximation for the D-form of the valine molecule, the binding energy of the first, the highest occupied orbital is −6.887 eV, and that of the 24th, the last considered, is −30.157 eV. The cross section of one-electron ionization is obtained by summing up all cross sections of one-electron ionization from each molecular orbital.

Figure 5 shows cross sections of one-electron ionization of the D- and DL-forms of valine molecules by electron impact at energies ranging from the threshold to 60 eV calculated in BEB-DFT models (10) and according to the Gryzinsky formula (11). These cross sections are compared with the measured total ionization cross section normalized at an energy of 8.8 eV by the value of the BEB-DFT cross section. At energies close to the threshold, the measured total ionization cross section corresponds to the ionization cross section of the parent molecule. As can be seen from Fig. 5, the ionization cross sections calculated in the same approximations for both forms of valine are close in magnitude. The Gryz-DFT cross sections systematically exceed the BEB-DFT cross sections and absolute measured values. The Gryz-DFT cross sections at energies from the threshold to the maximum grow faster than BEB-DFT cross sections and their behavior is similar to the measured one. The maximum values of ionization cross sections of the D-form of valine are the following (in 10^{-19} m^2): the experimental total cross-section is 4.053 at an energy of 30 eV; the BEB-DFT value is 2.882 at 67 eV while the Gryz-DFT value is 4.707 at 42.5 eV.

In Ref. [48], total ionization cross sections were measured for the amino acid molecules of glutamine ($C_5H_{10}N_2O_3$) and glutamic acid ($C_5H_9NO_4$). These cross sections were also normalized to the cross-sections one-electron ionization of the D-forms of the molecules calculated there by BEB-DFT and compared with the Gryz-DFT cross sections. The maximum values of the ionization cross sections of glutamine and glutamic acid molecules are the following (in 10^{-19} m^2 units): the total experimental values have two maxima (the—first one is 3.873 at an energy of 40 eV and 5.388 at 33.4 eV and the—second is 3.886 at 50 eV and 5.401 at 50.2 eV), the BEB-DFT calculated one is 3.252 at 70.0 eV and 3.050 at 72.5 eV while the Gryz-DFT one is 5.510 at 42.5 eV and 5.179 at 44.0 eV. Note that the Gryz-DFT cross sections of one-electron ionization of these molecules from the threshold to the maximum grow faster and their behavior is also similar to the measured data.

In Ref. [49], total electron ionization cross sections of adenine ($C_5H_5N_5$) and guanine ($C_5H_5N_5O$) biomolecules were measured. Their values in the maximum are as follows (in 10^{-19} m^2 units): adenine -2.8 ± 0.6 at an energy of 90 eV, guanine -3.2 ± 0.7 at an energy of 88 eV. It is seen that the ionization cross sections for these molecules are comparable in magnitude with our data. As for the behavior of the energy dependences of the total ionization cross sections, they have a form similar to ours.

In Ref. [50], total cross sections of one-electron ionization by electron impact of uracil ($C_4H_4N_2O_2$), thymine ($C_5H_6N_2O_2$), cytosine ($C_4H_5N_3O$), adenine ($C_5H_5N_5$), and guanine ($C_5H_5N_5O$) biomolecules were calculated in the BEB model. The maximum values of the cross sections (in 10^{-19} m^2 units) are as follows: guanine −2.184 at an energy of 80 eV, adenine −2.046 at 75 eV, thymine −1.761 at 82 eV; cytosine −1.658 at 80 eV,

uracil −1.457 at 85 eV. These data are seen to be in good agreement with those given in Ref. [49] and are close to ours.

In our opinion, the results obtained in our study as well as those of Refs. [49–51] confirm that such values of the maxima of ionization cross sections and their energy are inherent in biomolecules.

4 Conclusions

Mass spectra of the valine molecule in the mass number interval 0–120 Da were studied in the range of evaporation temperatures of the initial substance 300–440 K. A detailed analysis of the processes of formation of fragment ions of valine molecules by electron impact was carried out. It is shown that the difference in the structural forms of valine enantiomers is revealed in the mass spectra as a redistribution of child ion relative intensities. Information on the relative intensities of the mass peaks of the L-, DL-, and D-forms valine molecule obtained in different laboratories gives a more complete picture of the processes of formation of the fragment ions.

The total relative cross section of the valine molecule ionization by electrons was measured in the energy range of 5–60 eV. By approximating the near-threshold region of the energy dependence of the cross section, the ionization potential of the valine molecule was determined. This ionization potential value is compared with available experimental and theoretical data.

In the adiabatic approximation, we using standard quantum-chemical software packages calculated *ab initio* ionization potentials of three forms (D, DL, L) of the parent valine molecule. Their values coincide within the accuracy of 0.01 eV and are by 0.65 eV higher than the experimental one. The ionization potentials of these molecules also were estimated in the molecular orbital approximation.

Calculation of the cross sections for one-electron ionization of the D-, DL-, L-forms of the valine molecule by electron impact, carried out using the Binary-Encounter-Bethe model, enabled us to obtain the absolute values of the measured cross sections. The ionization cross sections for all forms of the valine molecule almost coincide with each other.

In conclusion, we would like to note that mass spectrometric studies of amino acids by electron impact in the gas phase provide a wealth of information about their unique properties, enable the magnitude of the degree of fragmentation in the process of interaction with electrons, to be determine the parameters of intermolecular bonds to be estimated.

Acknowledgements The authors are deeply grateful to their colleague Yu. M. Azhniuk for useful comments and assistance in preparing the article. One of the authors (E.R.) is grateful Ukrainian National Research Fund (Grant No. 2020.01/0009 Influence of ionizing radiation on the structure of amino acid molecules) for partial financial support.

Author contributions

A N Zavilopulo and A I Bulhakova contributed to experiments and analysis of their results. S S Demes, A V Vasiliev, and E Yu Remeta contributed to calculations and analysis of the results. All authors participated in the discussion of results and preparation of the manuscript.

Data Availability Statement This manuscript has associated data in a data repository. [Authors' comment: The data will be deposited in a repository on the web-site of the Institute of Electron Physics (http://iep.org.ua/)].

References

1. M. Inokuti, in *Atomic and Molecular Data Needed for Radiotherapy and Radiation Research TECDOC-799* (IAEA Press, Vienna, 1995)
2. L. Sanche, Radiat. Phys. Chem. **128**, 36 (2016). https://doi.org/10.1016/j.radphyschem.2016.05.008
3. N.M. Erdevdi, A.I. Bulhakova, O.B. Shpenik, A.N. Zavilopulo, Tech. Phys. Lett. **46**, 815 (2020). https://doi.org/10.1134/S1063785020080209
4. A.N. Zavilopulo, O.B. Shpenik, A.N. Mylymko, V.Y. Shpenik, Int. J. Mass Spectr. **441**, 1 (2019). https://doi.org/10.1016/j.ijms.2019.03.008
5. I.I. Fabrikant, S. Eden, N.J. Mason, J. Fedor, Adv. At. Mol. Opt. Phys. **66**, 546 (2017). https://doi.org/10.1016/bs.aamop.2017.02.002
6. Hu. Yongjun, E.R. Bernstein, J. Chem. Phys. **128**, 164311 (2008). https://doi.org/10.1063/1.2902980
7. C. Sonntag, in *The Chemical Basis for Radiation Biology* (Taylor & Francis Press, London, 1987)
8. V.V. Nikiforov, T.G. Suranova, T. Yu Chernobrovkina, Y.D. Yankovskaya, S.V. Burova, New coronavirus infection (Covid-19): clinical and epidemiological aspects. Russ. Arch. Intern. Med. Arch. **10**, 2 (2020). https://doi.org/10.20514/2226-6704-2020-10-2-87-93
9. B.K. Romanov, Coronavirus disease COVID-2019. Saf. Risk Pharmacother. **8**(1), 3 (2020). https://doi.org/10.30895/2312-7821-2020-8-1-3
10. J.F. Ward, in *Advances in Radiation Biology*. ed. by J.T. Lett, H.C. Adler (Academic Press, New York, 1977), p. 181
11. P. Papp, P. Shchukin, J. Kocisek, S. Matejcik, J. Chem. Phys. **137**, 105101 (2012). https://doi.org/10.1063/1.4749244
12. A. Zavilopulo, A. Bulhakova, S. Demes, E. Remeta, POSMOL 2021. Book of Abstracts 37 (2021)
13. S. Demes, A. Zavilopulo, A. Bulhakova, A. Vasiliev, E. Remeta, in *32nd International Conference on Photonic, Electronic and Atomic Collisions (ICPEAC 2021 Virtual format)* (Ottawa, Canada, 20–23 July 2021). Book of Abstracts 287

14. S. Denifl, I. Mähr, F. Ferreira da Silva, F. Zappa, T.D. Märk, P. Scheier, Eur. Phys. J. D **51**, 73 (2009). https://doi.org/10.1140/epjd/e2008-00092-4
15. N. Weinberger, S. Ralser, M. Renzler, M. Harnisch, A. Kaiser, S. Denifl, D.K. Böhme, P. Scheier, Eur. Phys. J. D **70**, 91 (2016). https://doi.org/10.1140/epjd/e2016-60737-1
16. A.N. Zavilopulo, E.A. Mironets, A.S. Agafonova, Instrum. Exp. Tech. **55**, 65 (2012). https://doi.org/10.1134/S0020441211060315
17. U. Meierhenrich, in *Amino Acids and the Asymmetry of Life* (Springer, Berlin, 2008)
18. O.V. Smirnov, A.A. Basalaev, V.M. Boitsov, SYu. Vyaz'min, A.L. Orbeli, M.V. Dubina, Technical Physics **59**, 1698 (2014). https://doi.org/10.1134/S1063784214110231
19. A.N. Zavilopulo, A.I. Bulhakova, Tech. Phys. Lett. **45**, 1252 (2019). https://doi.org/10.1134/S1063785019120290
20. NIST Standard Reference Database. http://www.webbook.nist.gov
21. Spectral Database for Organic Compounds SDBS. https://sdbs.db.aist.go.jp
22. H.-W. Jochims, M. Schwell, J.-L. Chotin, M. Clemino, F. Dulieu, H. Baumgärtel, S. Leach, Chem. Phys. **298**, 279 (2004). https://doi.org/10.1016/j.chemphys.2003.11.035
23. G. Junk, H. Svec, J. Am. Chem. Soc. **85**, 839 (1963). https://doi.org/10.1021/ja00890a001
24. X. Song, J. Li, H. Hou, B. Wang, J. Chem. Phys. **125**, 094301 (2006). https://doi.org/10.1063/1.2347711
25. M. Nuevo, U.J. Meierhenrich, G.M. Munoz Caro, E. Dartois, L. d'Hendecourt, D. Deboffle, G. Auger, D. Blanot, J.-H. Bredehoft, L. Nahon, Astron. Astrophys. **457**, 741 (2006)
26. J. Bonner, Y.A. Lyon, C. Nellessen, R.R. Julian, J. Am. Chem. Soc. **139**, 10286–10293 (2017). https://doi.org/10.1021/jacs.7b02428
27. J. Tamulienė, L. Romanova, V. Vukstich et al., Lith. J. Phys. **58**, 135 (2018)
28. A. Ostroverkh, A. Zavilopulo, O. Shpenik, Eur. Phys. J. D **73**, 38 (2019). https://doi.org/10.1140/epjd/e2019-90532-3
29. M.Y. Choi, R.E. Miller, J. Am. Chem. Soc. **128**(22), 7320 (2006). https://doi.org/10.1021/ja060741l
30. A.N. Zavilopulo, O.B. Shpenik, P.P. Markush, E.E. Kontrosh, Tech. Phys. **60**, 957 (2015). https://doi.org/10.1134/S1063784215070282
31. L. Klasinc, Electron Spectrosc. Relat. Phenom. **8**, 161 (1976). https://doi.org/10.1016/0368-2048(76)80018-7
32. R.S. Berry, S. Leach, Adv. Electron. Electron Phys. **57**, 1 (1981)
33. D.M. Close, J. Phys. Chem. A **115**(13), 2900 (2011). https://doi.org/10.1021/jp200503z
34. D. Dehareng, G. Dive, Int. J. Mol. Sci. **5**(11), 301 (2004). https://doi.org/10.3390/i5110301
35. M.J. Frisch, G.W. Trucks, H.B. Schlegel, G.E. Scuseria, M.A. Robb, J.R. Cheeseman, G. Scalmani, V. Barone, B. Mennucci, G.A. Petersson, *Gaussian 09, Revision E.01* (Gaussian Inc., Wallingford CT, 2009)
36. O. Shpenik, A. Zavilopulo, E. Remeta, S. Demes, M. Erdevdy, Ukr. J. Phys. **65**(7), 557 (2020). https://doi.org/10.15407/ujpe65.7.557
37. ShSh. Demesh, A.N. Zavilopulo, O.B. Shpenik, EYu. Remeta, Tech. Phys. **85**(6), 44 (2015). https://doi.org/10.1134/S1063784215060067
38. ShSh. Demesh, EYu. Remeta, Eur. Phys. J. D **69**, 168 (2015). https://doi.org/10.1140/epjd/e2015-50636-4
39. National Center for Biotechnology Information. PubChem Database. Glutamine, CID=5961 https://pubchem.ncbi.nlm.nih.gov/compound/Glutamine Accessed on Apr. 29, 2020
40. National Center for Biotechnology Information. PubChem Database. Glutamic acid, CID=33032 https://pubchem.ncbi.nlm.nih.gov/compound/Glutamic-acid Accessed on Apr. 29, 2020
41. M.D. Hanwell, D.E. Curtis, D.C. Lonie, T. Vandermeersch, E. Zurek, G.R. Hutchison, J. Cheminform. **4**, 17 (2012). https://doi.org/10.1186/1758-2946-4-17
42. E. Illenberger, J. Momigny, in *Gaseous Molecular Ions. Topics in Physical Chemistry* (Vol. 2, Steinkopff-Verlag, Heidelberg, 1992). p. 346
43. J. Maruani, E.J. Brändas, in *Progress in Theoretical Chemistry and Physics* (Springer, Cham, 2013) https://doi.org/10.1007/978-3-319-01529-3
44. J.H. Gross, in *Mass Spectrometry* (Springer, Berlin, 2011)
45. K. Yong-Kim, M.E. Rudd, Phys. Rev. A **50**(5), 3954 (1994). https://doi.org/10.1103/physreva.50.3954
46. K. Yong-Kim, K.K. Irikura, M.A. Ali, J. Res. Natl. Inst. Stand. Technol. **105**(2), 285 (2000). https://doi.org/10.6028/jres.105.032
47. H. Tanaka, M.J. Brunger, L. Campbell, H. Kato, M. Hoshino, A.R.P. Rau, Rev. Mod. Phys. **88**, 025004 (2016). https://doi.org/10.1103/RevModPhys.88.025004
48. M. Gryzinski, Phys. Rev. **138**(2A), A336 (1965). https://doi.org/10.1103/PhysRev.138.A336
49. I.I. Shafranyosh, YuYu. Svyda, M.I. Sukhoviya, M.I. Shafranyosh, B.F. Minaiev, H.V. Barishnikov, V.A. Minaiev, Tech. Phys. **85**(10), 16 (2015). https://doi.org/10.1134/S1063784215100278
50. P. Mozejko, L. Sanche, Radiat. Environ. Biophys. **42**, 201 (2003). https://doi.org/10.1007/s00411-003-0206-7
51. A.N. Zavilopulo, S. Demes, EYu. Remeta, A.I. Bulhakova, Ukr. J. Phys. **66**(9), 745 (2021)